Macromolecular Reaction Engineering

Modeling the Synthesis of Butyl Methacrylate Macromonomer by Sequential ATRP-CCTP

--Manuscript Draft--

Manuscript Number:	mren.201800062R1
Full Title:	Modeling the Synthesis of Butyl Methacrylate Macromonomer by Sequential ATRP-CCTP
Article Type:	Full Paper
Section/Category:	Special Issue: Innovative processes and products (by invitation only)
Keywords:	Low Đ macromonomer; ATRP; Cobalt chain transfer polymerization; modeling and simulation; radical polymerization
Corresponding Author:	Robin A. Hutchinson, Prof. Queen's University Kingston, Ontario CANADA
Corresponding Author Secondary Information:	
Corresponding Author's Institution:	Queen's University
Corresponding Author's Secondary Institution:	
First Author:	Robin A. Hutchinson, Prof.
First Author Secondary Information:	
Order of Authors:	Robin A. Hutchinson, Prof.
	Mingmin Zhang
Order of Authors Secondary Information:	
Abstract:	The atom transfer radical polymerization of butyl methacrylate mediated by Cu(I)Br/N,N,N′,N″,N″-pentamethyldiethylenetriamine in anisole at 70°C with the subsequent addition of bis(difluoroboryldiphenylglyoximato)cobalt(II) after 2 h is modeled using Predici® software, to gain additional insight to the system used experimentally to produce macromonomer chains with narrow dispersity. The mechanistic model, using kinetic coefficients from the literature and activation and deactivation rate coefficients estimated from this work, provides a good representation of experimental results. The simulations demonstrate that the time (conversion) at which cobalt chain transfer agent is added to the system is critical to control the number average molar mass of the final product, and also confirm that chains of higher length in the final product are more likely to be non-functionalized, in agreement with experimental observations. The model predicts the production of a significant fraction of macromonomer oligomers with lengths of 1-3 units, also consistent with experiments.
Additional Information:	
Question	**Response**
Please submit a plain text version of your cover letter here.	We submit this manuscript as part of the planned issues from the ECI "Polymer Reaction Engineering X" conference held in Punta Cana in May 2018. The manuscript can be moved to either special issue, as it discusses modeling of a novel ATRP-CCTP process.
Do you or any of your co-authors have a conflict of interest to declare?	No. The authors declare no conflict of interest.

Modeling the Synthesis of Butyl Methacrylate Macromonomer by Sequential ATRP-CCTP[a]

*Mingmin Zhang, Robin A. Hutchinson**

M. Zhang, Prof. R. A. Hutchinson
Department of Chemical Engineering, Queen's University,
19 Division St., Dupuis Hall, Kingston, Ontario, K7L 3N6, Canada
E-mail: robin.hutchinson@queensu.ca

The atom transfer radical polymerization of butyl methacrylate mediated by Cu(I)Br/*N*,*N*,*N*′,*N*″,*N*″-pentamethyldiethylenetriamine in anisole at 70 ℃ with the subsequent addition of bis(difluoroboryldiphenylglyoximato)cobalt(II) after 2 h is modeled using Predici® software, to gain additional insight to the system used experimentally to produce macromonomer chains with narrow dispersity. The mechanistic model, using kinetic coefficients from the literature and activation and deactivation rate coefficients estimated from this work, provides a good representation of experimental results. The simulations demonstrate that the time (conversion) at which cobalt chain transfer agent is added to the system is critical to control the number average molar mass of the final product, and also confirm that chains of higher length in the final product are more likely to be non-functionalized, in agreement with experimental observations. The model predicts the production of a significant fraction of macromonomer oligomers with lengths of 1-3 units, also consistent with experiments.

Supporting Information is available online from the Wiley Online Library or from the author.

1. Introduction

In catalytic chain transfer polymerization (CCTP), a small amount of cobalt chain transfer (CCT) agent is added to radical polymerization to produce polymers containing unsaturated end groups[1-3] with the so-called macromonomer used for further post-reaction.[4-7] As the chains are produced continuously during the reaction by decomposition of a thermal initiator, the macromonomers synthesized by CCTP chemistry have a dispersity (Đ) close to 2.[7-9]

Atom transfer radical polymerization (ATRP) is a type of reversible deactivation radical polymerization (RDRP) used to create polymers of controlled molecular weight and architecture (block, gradient, star) with high livingness and low Đ (Đ< 1.4); all of the chains are initiated at the beginning of the reaction, with their growth regulated by reversible radical capture involving a Cu(I)-Cu(II) activation/deactivation cycle that minimizes the occurrence of bimolecular termination.[10,11] It was demonstrated that P(MMA) macromonomer with high vinyl end group functionality and low Đ could be synthesized through the combinination of both techniques, with the CCT agent bis{μ-[(2,3-butanedione dioximato) (2-) O:O']} tetrafluorodiborato(2-) N, N', N'', N''' cobalt (II) (CoBF) or 5,10,15,20-tetraphenyl-21H, 23H-porphine cobalt(II) Co(tpp) (Figure 1) added towards the end of polymerization to add terminal double bonds to the uniform chains mediated by ATRP chemistry.[12] Very recently, low Đ P(BMA) was synthesized through this sequential ATRP-CCTP technique using bis(difluoroboryldiphenylglyoximato)cobalt(II) (CoPheBF, Figure 1) as the CCT agent; the study showed that lowering the dispersity of macromonomer by this strategy improved its efficiency as a dispersant in nonaqueous dispersion polymerization compared to a similar material with a dispersity of two.[8]

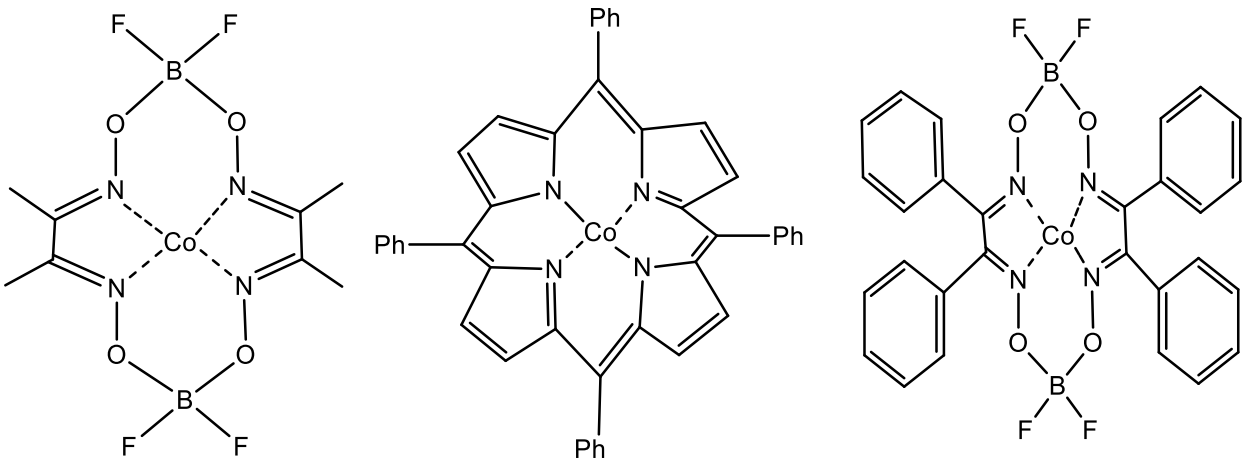

Figure 1. Structure of cobalt chain transfer reagents. CoPheBF was used in this work.

It is the goal of this work to develop a first model of the ATRP-CCTP system by combining the known mechanisms of each chemistry. Several papers describe modeling the ATRP of different monomers, typically styrene[13-18] and its copolymerization with acrylates.[19,20] In the traditional ATRP process (Scheme 1), radicals are generated from a Br-capped alkyl radical (either initiator or a growing polymer chain) through a reversible redox process, catalyzed by a transition metal such as Cu (the focus of this work),[21] Ru,[22] or Fe[23] that allows for much faster deactivation of growing radicals (k_{da}) relative to their formation by activation (k_a). An equilibrium is established between the two processes (k_a/k_{da} =10^{-4} to 10^{-8})[24] to keep the radical concentration low, leading to controlled chain growth with a suppressed rate of bimolecular radical termination.

Later, a modified ATRP technique named activator regenerated by electron transfer (ARGET) ATRP[25] was developed. The addition of a reducing agent such as tin(II)-ethylhexanoate to promote the conversion of Cu(II) to Cu(I) activator allowed the reaction to proceed with a much lower amount of Cu(II)Br_2 catalyst ($<$ 300 ppm) compared with traditional ATRP, which requires higher Cu levels ($>\sim$ 5000 ppm with respect to monomer on a molar basis) to well control the growth of the polymer chains.

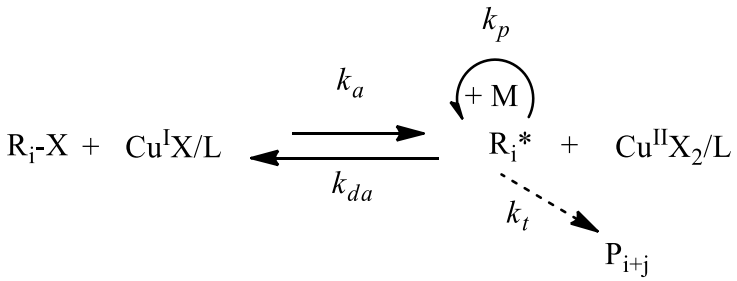

Scheme 1. Mediation of Radical Chain Growth by Normal ATRP

In addition to the standard mechanisms of radical polymerization, the modeling of ARGET ATRP includes the activation, deactivation and reduction reactions, with the associated rate coefficients normally estimated by the specific experimental data.[26,27] These previous efforts will be used as a starting point for the representation of ATRP chemistry in the combined ATRP-CCTP model developed in this work.

Models of radical CCTP of styrene[28] and methacrylates can also be found in the literature, with a focus on methyl methacrylate[29,30] and its copolymerization.[31-33] In addition to initiation, propagation and termination, the generally accepted mechanism for CCTP, used in this work, consists of two reactions – hydrogen abstraction and reinitiation. In the first reaction (Equation I in Scheme 2), a growing radical R_i^* (subscript *i* represents chain length) reacts with a Co(II) complex to produce a macromonomer, also of length *i*, and a Co(III)H intermediate. In the subsequent reinitiation reaction (Equation II), the Co(III)H intermediate reacts with a monomer to yield a monomeric radical (R_1^*) and regenerates the Co(II) complex.[33] As a macromonomer of chain length of 1 is simply monomer, a monomer renewal mechanism (Equation III) is required in order to correctly model the conversion profile.[32]

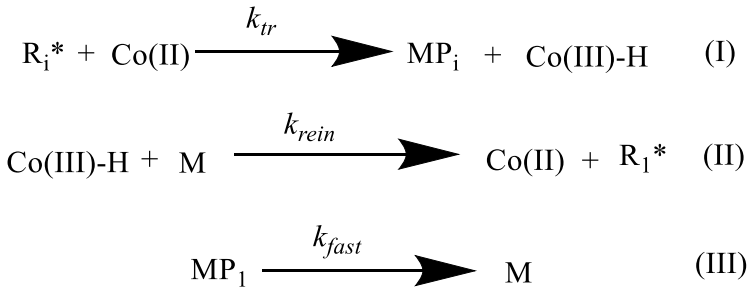

Scheme 2. Formation of Polymer Chains with Terminal Double Bonds (MP_i) by Cobalt Chain-Transfer Polymerization

In this work, we combine these mechanisms to model, for the first time, the sequential ATRP-CCTP process, using Predici® software to develop the representation of ATRP of BMA in anisole at 70 ℃ mediated with Cu(I)Br/PMDETA, EBiB as the initiator and CoPheBF as the CCT agent added at the latter stages of the reaction. Starting from estimates from literature, the activation and deactivation coefficients are adjusted to provide a representation of the experimentally measured conversion, average chain-length and dispersity profiles, with the influence of the mode of termination on the production of terminal double bonds during the ATRP reaction also investigated. The model is then used to explore the influence of operating conditions on the extent of terminal double-bond (TDB) functionalization achieved in the system, as well as to explore whether the high molar mass polymer chains in the distribution are more likely to be dead chains terminated by combination, a hypothesis put forth to explain results obtained when using the low Đ macromonomer P(BMA) as the dispersant in nonaqueous dispersion polymerization.[8]

2. Experimental Section

2.1 Materials

n-Butyl methacrylate (BMA, 99%), deuterochloroform ($CDCl_3$, 99.8 atom% D), copper(I) bromide (Cu(I)Br, 98%), anisole (99%), ethyl α-bromoisobutyrate (EBiB, 98%), N,N,N′,N″,N″-

pentamethyldiethylenetriamine (PMDETA, 99%) and tetrahydrofuran (THF, 99%) were purchased from Sigma Aldrich and used as received. Methanol (99.8%) purchased from ACP Chemicals was also used as received. Water was purified using a Millipore Synergy water purification system equipped with SynergyPak purification cartridges. Bis(difluoroboryldiphenylglyoximato)cobalt(II) (CoPheBF) was supplied by Axalta Coating Systems.

2.2 Batch ATRP of BMA

The experimental procedures and recipe were outlined in the previous paper.[8] The batch reaction was conducted in a stirred vessel controlled at 70 C in 50 wt% anisole with initial molar ratios of $[BMA]_0$:$[EBiB]_0$:$[CuBr]_0$:$[PMDETA]_0$ of 42:1:0.4:0.8. After stopping the reaction by exposure to the air, an alumina column was used to remove the catalyst and residual initiator, with methanol/water (1:1 v/v) used to precipitate the product. The separated polymer was first air-dried and then dried in a vacuum oven for 72 h at 80 ℃.

2.3 Sequential ATRP-CCTP of BMA

The reaction recipe and conditions are the same as previously described,[8] with the CoPheBF chain transfer agent added to the system after the ATRP reaction had proceeded for 2 h, corresponding to roughly 80% monomer conversion. The reaction was stopped at 4h by exposure to the air and product isolated as described above. SEC and NMR was used to determine that 83.3 mol% (5400 Da, Đ = 1.25) of the final product contains TDB, i.e., is macromonomer.

2.4 Characterization

Average molar masses and molar mass distributions of samples were measured by size exclusion chromatography (SEC) using a Waters 2960 separation module with 4 Styragel columns (HR 0.5, 1, 3, 4) followed by a Waters 410 differential refractometer (DRI) operated at 35 ℃**,** with THF as eluent at a flow rate of 0.3 $mL \cdot min^{-1}$. The DRI detector was calibrated by 10 low dispersity

polystyrene standards with MW from 870 Da to 355 000 Da. MW values of the P(BMA) samples are reported after applying universal calibration procedures with Mark-Houwink parameters for PS ($K = 11.4\times10^{-5}$ dL·g^{-1}, $\alpha = 0.716$)[34] and for P(BMA) ($K = 14.8\times10^{-5}$ dL·g^{-1}, $\alpha = 0.664$).[34]

A Bruker Avance-500 MHz NMR spectrometer at 25 ℃ was used to characterize the P(BMA) macromonomer samples dissolved in deuterated chloroform ($CDCl_3$) at a concentration of 5 mg·mL^{-1}. The ratio of terminal double-bond to repeat unit ester protons (-OCH_2-) was calculated as detailed in Supporting Information.

3. Results and Discussion

3.1 Mechanistic Model Development

The model is developed in two stages, starting with the representation of ATRP of BMA and the estimation of activation and deactivation rate coefficients and the fraction of termination by disproportionation (k_{td}/k_t) from the experimental data, followed by the development of the full ATRP-CCTP model based on the mechanisms proposed in the literature, as presented in Table 1.

Most of the kinetic parameters summarized in Table 1 are taken from previous literature. The density of BMA monomer[34] is ρ_{BMA} = 0.91454-9.64 × 10^{-4} T/℃ g·cm^{-3}, polymer density[41] is ρ_P = 1.19 – 8.07 × 10^{-4} T/℃ g·cm^{-3}, and the density of anisole is $\rho_{anisole}$ =0.995 g·cm^{-3} neglecting the temperature dependency. While chain-length dependency of termination was not considered in this model, the k_t value used is a chain-length-averaged value calculated from the implementation of the composite-model by Payne et al.[27] In addition to radical species (R_i^*), three different distributions of chains are tracked by the model: dormant (bromine capped) chains (R_iX), dead chains (P_i), and macromonomer chains (MP_i) formed by termination by disproportionation or by hydrogen abstraction through the CCT mechanism. In this work, the reported M_n and Đ values are

calculated by summing up these distributions. As mentioned in the experimental section, the SEC calibration range is from 870 to 355 000 Da and the polymer samples were precipitated and dried in vacuum oven at 80 ℃ for 72 h before SEC characterization. Thus, the contribution of chains of lengths 1-3, outside of the SEC-calibration region, are subtracted from the distributions before summation, as also done for previous models developed to represent ARGET-ATRP[27] and CCTP.[32]

The Matyjaszewski research group has greatly contributed to the understanding of the ATRP mechanism, measuring both k_a and K_{ATRP},[35-38] with the corresponding deactivation rate coefficient estimated by $K_{ATRP} = {k_a}/{k_{da}}$. Specifically, Nanda and Matyjaszewski[35] reported the effect of the penultimate unit on the activation rate coefficient, determining that the activation rate coefficient for ATRP dormant polymeric species (k_a) is at least 10 times larger than that for ATRP initiator ($k_{a,0}$). This difference in the activation kinetics of initiator and dormant chains was applied by Payne et al. to model the ARGET-ATRP of BMA[27,39] and provide good agreement between the experimental and simulation results. As this work utilizes the same monomer BMA, ATRP initiator EBiB, Cu(I)Br as the catalyst in the activation reaction, and anisole as the solvent, the same $k_{a,0}$ value of 3.25 L·mol^{-1}·s^{-1} at 70 ℃ is used. Note, however, that while the ARGET-ATRP study used tris(2-pyridylmethyl)amine (TPMA) as ligand, here we use PMDETA; thus, the activation energy E_a = 2.77× 10^4 J·mol^{-1} reported by Seeliger and Matyjaszewski[37] for EBiB activation (Cu(I)Br/PMDETA, acetonitrile as solvent) over the temperature range of −40 ℃ to 40 ℃ is used to relate this $k_{a,0}$ value to K_{ATRP} values reported at different temperatures.

Table 1. Mechanisms and 70 ℃ rate coefficients used to model the sequential ATRP-CCTP of BMA in anisole, with EBiB as ATRP initiator, Cu(I)X/L as activator and CoPheBF as CCT agent, where X = Br, L = PMDETA; Subscript "0" relates to ATRP initiator.

Mechanism	Parameter	70 °C Value ($L \cdot mol^{-1} \cdot s^{-1}$)	Ref.
ATRP activation/deactivation			
$R_oX + Cu^IX/L \xrightarrow{k_{a,0}} R_o^* + Cu^{II}X_2/L$	$k_{a,0}$	3.25	27
$R_iX + Cu^IX/L \xrightarrow{k_a} R_i^* + Cu^{II}X_2/L$	k_a	42.5	This work
$R_o^* + Cu^{II}X_2/L \xrightarrow{k_{da,0}} R_oX + Cu^IX/L$	$k_{da,0}$	2.7×10^7	This work
$R_i^* + Cu^{II}X_2/L \xrightarrow{k_{da}} R_iX + Cu^IX/L$	k_{da}	1.57×10^7	This work
Propagation			
$R_o^* + M \xrightarrow{k_{p,0}} R_1^*$	$k_{p,0}$	1.23×10^3	27
$R_i^* + M \xrightarrow{k_p} R_{i+1}^*$	k_p	1.23×10^3	27
Termination by disproportionation			
$R_i^* + R_j^* \xrightarrow{k_{td,ij}} P_i + MP_j$	$k_{td,ij} = 0.75k_t$	6.75×10^{7a}	27 This work
Termination by combination			
$R_i^* + R_j^* \xrightarrow{k_{tc,ij}} P_{i+j}$	$k_{tc,ij} = 0.25k_t$	2.25×10^{7a}	27 This work
CCT reactions			
$R_i^* + Co(II) \xrightarrow{k_{tr}} MP_i + Co(III)\text{-}H$	k_{tr}	2.85×10^{7b}	32
$Co(III)\text{-}H + M \xrightarrow{k_{rein}} Co(II) + R_1^*$	k_{rein}	1.0×10^3	32
Monomer renewal			
$MP_1 \xrightarrow{k_{fast}} M$	k_{fast} (s^{-1})	1.0×10^3	This work

[a] Here $\lambda = {k_{td}}/{k_t} = 0.75$ and $k_t = 9\times 10^7$ $L \cdot mol^{-1} \cdot s^{-1}$ (k_t is a chain-length-averaged value calculated from Ref. 27); [b] $k_{tr} = C_{tr} \times k_p = 2.3\times 10^4 \times 1.23\times 10^3 = 2.83\times 10^7$ $L \cdot mol^{-1} \cdot s^{-1}$

From the modeling perspective, the main difference between this BMA ATRP system and Payne's ARGET-ATRP study is the effect of ligand choice (PMDETA vs. TPMA) on the activation and deactivation rate coefficients. In order to estimate the values of k_a, $k_{da,0}$ and k_{da} using Predici® software, it is very important to provide reasonable bounding limits.

It can be inferred that k_a in the current system at 70 ℃ is about 10 times larger than $k_{a,0}$ = 3.25 L·mol^{-1}·s^{-1} but much smaller than $k_{a,TPMA}$ = 240 L·mol^{-1}·s^{-1} reported by Payne et al.;[27] this latter estimate is based on Tang and Matyjaszewski's study[36] of the effect of ligand choice on the activation rate coefficient (k_a) of EBiB in acetonitrile (MeCN) that found $k_{a,TPMA}$ is 10 to 100 times larger than $k_{a,PMDETA}$. It can also be assumed that $K_{ATRP,0}$ of the current system is close to the value of 1.35×10^{-7} suggested from Payne et al., and that $K_{ATRP,PMDETA}$ is bounded by the $K_{ATRP,TPMA}$ value of 2×10^{-5} used by Payne et al. and 1×10^{-8} inferred from the study on the ligand effect on the ATRP equilibrium constant using EBiB, Cu(I)Br in MeCN at 22 ℃ with $K_{ATRP,PMDETA} = 7.5 \times 10^{-8}$ and $K_{ATRP,TPMA} = 9.6 \times 10^{-6}$.[38] This range of values is supported by a more recent study[40] reporting that $K_{ATRP,PMDETA}$ is 9.8×10^{-8} and $K_{ATRP,TPMA}$ is 2.0×10^{-5} using EBiB and Cu(I)Br in MeCN at 25 ℃, based on extrapolation from measured values at pressures between 50 and 2500 bar. The corresponding bounding ranges of $k_{da,0}$ and k_{da} in this work are estimated using these ranges for $K_{ATRP,0}$ and $K_{ATRP,PMDETA}$. More specifically, at first k_a and $k_{da,0}$ were estimated simultaneously by Predici® with the values (with 95% confidence interval) determined as 42.5±21.2 L·mol^{-1}·s^{-1}and $2.7\pm1.9\times 10^{7}$ L·mol^{-1}·s^{-1}respectively at 70 ℃, giving equal weighting to the conversion, M_n, and Đ experimental responses. The 70 ℃ value of k_{da} was then estimated to be $15.7\pm4.1 \times 10^{6}$ L·mol^{-1}·s^{-1}. The only other rate coefficient estimated in this

work is the fraction of termination by disproportionation for BMA in anisole, whose ratio λ = k_{td}/k_t was varied from 0.65[41] to 0.90,[32] as discussed later.

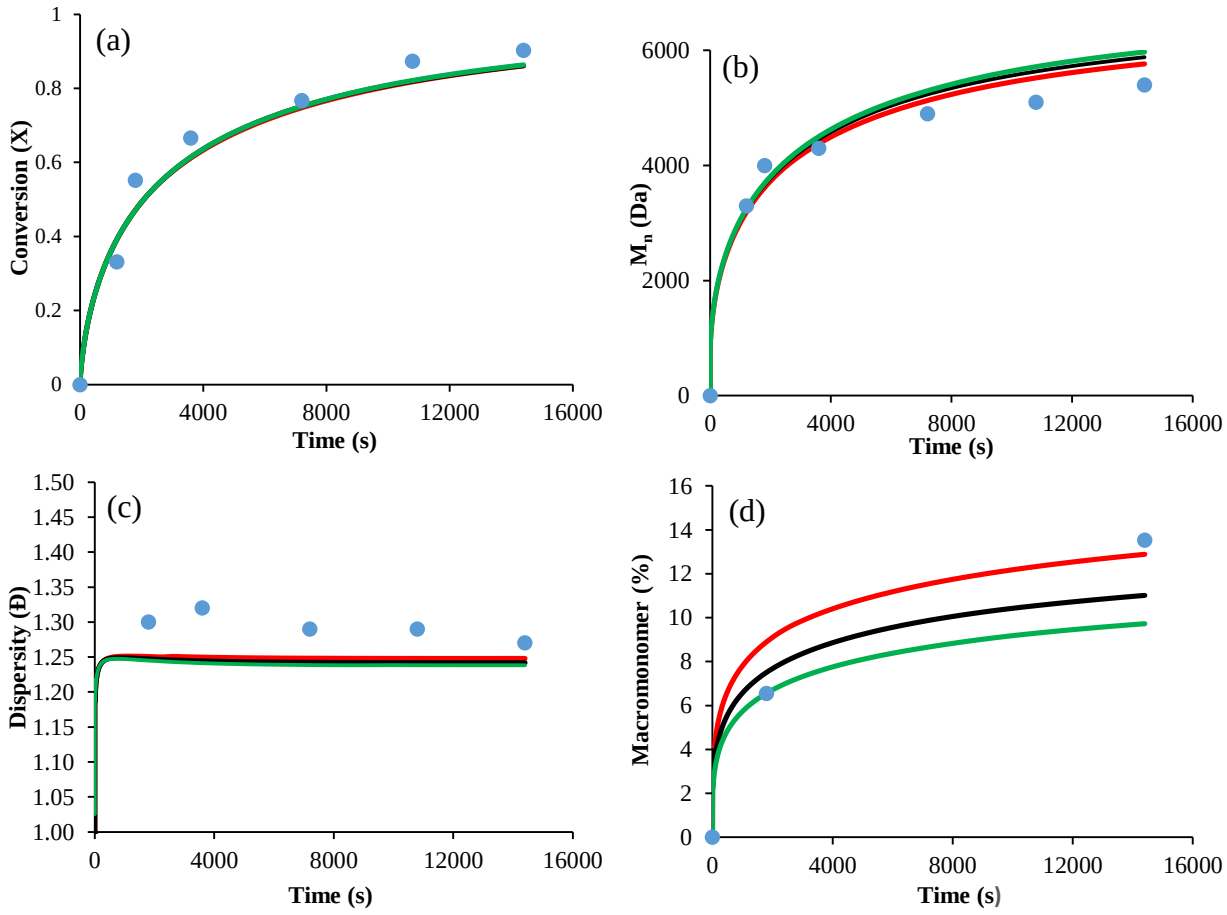

Figure 2. Simulated (lines) and experimental (points) profiles of (a) conversion, (b) number average molar mass M_n, (c) dispersity Đ, and (d) percentage of chains that are terminated by double bonds for batch ATRP of BMA with $[M]_0$:$[I]_0$:$[CuBr]_0$:$[L]_0$ = 42:1:0.4:0.8 in 50 wt% anisole at 70 °C. Kinetic parameters for simulation are given in Table 1 (k_t = 9× 10^7 L·mol^{-1}·s^{-1}, red - k_{td} = 0.9k_t, black - k_{td} = 0.75k_t, green - k_{td} = 0.65k_t).

The simulation results using the best-fit estimates of ATRP activation and deactivation rate coefficients are compared to the experimental results in Figure 2. In this series of simulations, the fraction of termination by disproportionation is varied. The value of λ does not affect the calculated conversion (X), M_n, and dispersity greatly since the fraction of dead chains is low. However, the

value influences the calculated percentage of macromonomer (as a mole fraction of total chains) in the system, which has been experimentally estimated using ^{1}H NMR. As mentioned previously, the values of λ used in previous simulations ranges from 0.65 to 0.9,[32,41,42] with the lower value of 0.65 more in line with experimental estimations for methacrylate monomers. The simulations shown in Figure 2 suggest a value of 0.9 provides a better fit of the TDB level measured at 14400 s, while the value of 0.65 provides a better estimate of the earlier measurements. As a compromise, the value of 0.75 was chosen for the remainder of the simulations.

The sensitivity of model predictions to the values of $k_{da,0}$, k_a and k_{da} was also examined. For the purpose of conciseness, only the sensitivity with respect to k_a is shown, with the sensitivity to $k_{da,0}$ and k_{da} presented as Supporting Information. The simulation results shown in Figure 3 compare the profiles generated with the k_a value raised and lowered by an order of magnitude relative to the best fit value of 42.5 L·mol^{-1}·s^{-1}. It can be seen that the experimental data can only be matched with this best-fit value, as the higher value leads to the predicted loss of control (high dispersity due to termination of radicals), and the lower value results in a lower rate of conversion (with better control) than observed experimentally. Although further experiments with varying initiator and mediator concentrations would be required to verify the complete set of activation/deactivation kinetics estimated, the set of parameters selected are within the range of accepted values from literature and provide an excellent description of experimental results. The acquisition of additional data would also allow the consideration of chain-length dependent termination, shown to be important in previous ATRP modeling efforts.[27]

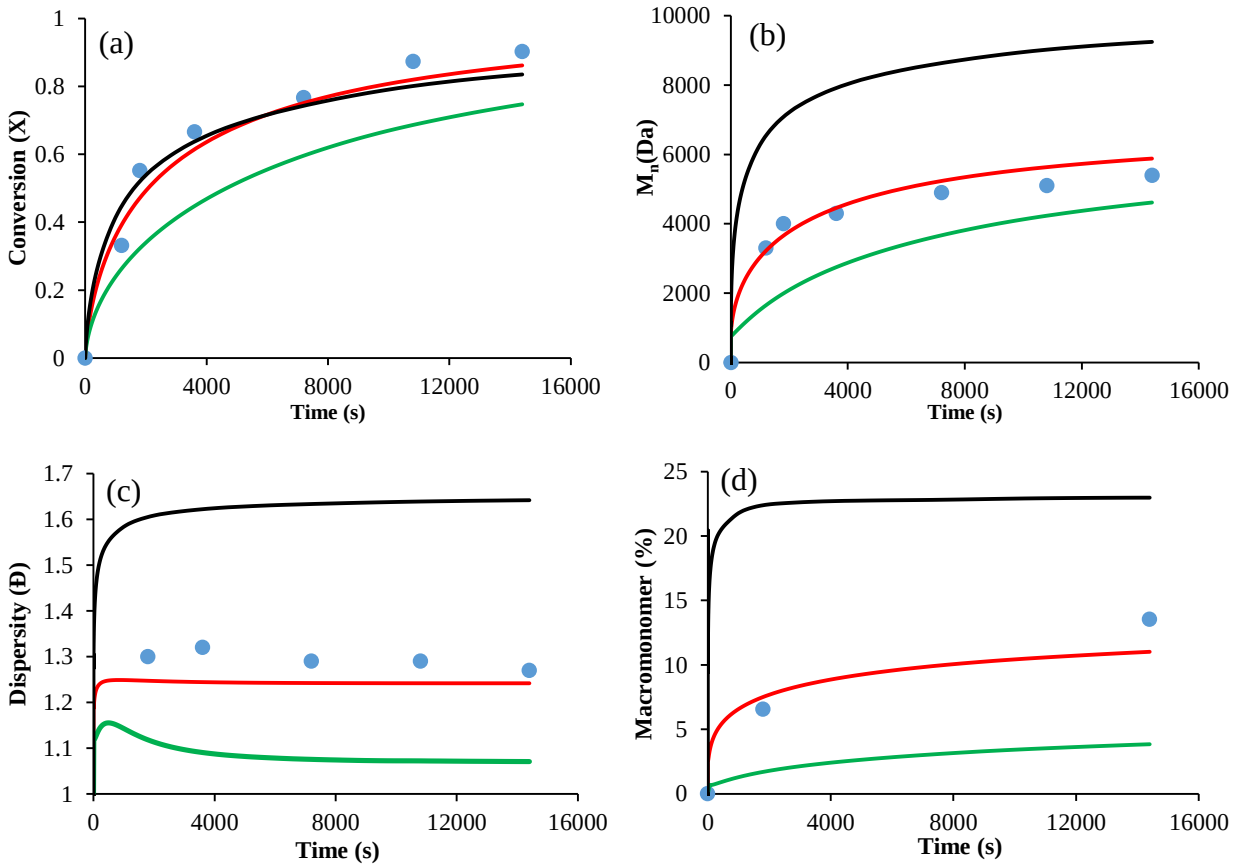

Figure 3. The sensitivity of simulated profiles (lines) for (a) conversion, (b) number average molar mass M_n, (c) dispersity Đ, and (d) percentage of chains that are terminated by double bonds to the value of k_a set at 425 L·mol^{-1}·s^{-1} (black), the best-fit value of 42.5 L·mol^{-1}·s^{-1} (red) and 4.25 L·mol^{-1}·s^{-1} (green). Points are experimental results for batch ATRP of BMA with $[M]_0$:$[I]_0$:$[CuBr]_0$:$[L]_0$ = 42:1:0.4:0.8 in 50 wt% anisole at 70 ℃. The remaining kinetic parameters used in the simulation are given in Table 1.

In the second step, the model is used to represent the sequential ATRP-CCTP of BMA. Thus, the Table 1 mechanisms and rate coefficients relating to the CCT agent become important. The coefficient of catalytic chain transfer ($C_{tr} = {k_{tr}}/{k_p}$) and reinitiation k_{rein} were used without modification from the previous modeling study of BMA CCTP[32] and the constant of monomer renewal k_{fast} was set at 1×10^3 s^{-1}, as increasing its value to 1×10^5 s^{-1} had no effect on simulated profiles, but greatly increased the time required to complete the simulation due to numerical difficulties in maintaining the concentration of MP_1 at a very low, but positive, value.

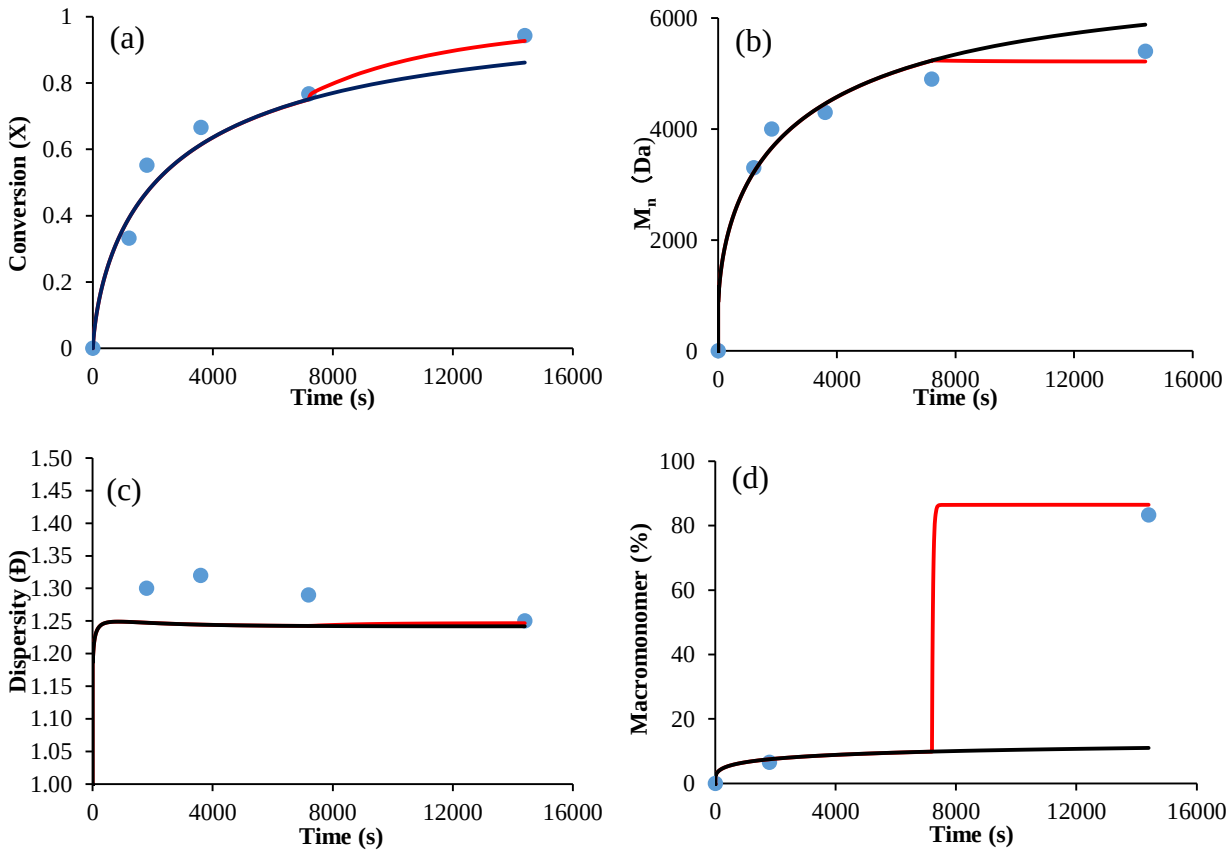

Figure 4. Simulated (lines) and experimental (points) profiles of (a) conversion, (b) number average molar mass M_n, (c) dispersity Đ, and (d) percentage of chains that are terminated by double bonds for sequential ATRP of BMA with $[M]_0$:$[I]_0$:$[CuBr]_0$:$[L]_0$ = 42:1:0.4:0.8 in 50 wt% anisole at 70 ℃. The CoPheBF (44.8 mg) is added at 7200 s. Kinetic parameters for simulation are given in Table 1, with red lines for the simulation of the sequential ATRP-CCTP, and black lines for the simulation of the corresponding ATRP reaction without addition of Cobalt chain transfer agent.

The simulation of the sequential ATRP-CCTP experiment is compared in Figure 4 to experimental results as well as to the simulation of the ATRP reaction without addition of CCT agent. After the addition of CoPheBF at 7200 s, the simulation indicates a slight increase in rate, as reflected in the change in the slope of the conversion profile (Figure 4a). The number average molar mass and dispersity values are predicted not to noticeably change after addition of CCT agent at 7200 s (Figure 4b and 4c). The termination of chains by CCT leads to a significant and almost instantaneous increase in the fraction of macromonomers in the system compared with the

corresponding ATRP process. It should be remembered that the properties of the polymer – number average MW, dispersity, and also % macromonomer – are calculated after subtracting out contributions from chains of lengths 1 to 3. Thus, the predicted increase in monomer conversion has no influence on the predicted chain length, as the additional polymer formed consists entirely of low MW oligomeric material, as discussed below.

3.2 Composition of Final Product

In the experimental study,[8] it was hypothesized that a higher proportion of the longer product chains are not macromonomers, as the soluble polymer recovered after dispersion polymerization contained a greater fraction of high MW material compared to the MMD of the original distribution. As Predici® provides a representation of the full MMD, this hypothesis can be investigated by comparing the distributions of the three different types of polymer chains tracked by the simulation, macromonomomer, bromine-capped chains, and terminated saturated chains (dead chains); the later two distributions are combined to make up the material termed herein as "polymer without vinyl endgroups".

As mentioned previously, the simulated distributions and their averages are presented after subtracting out the contribution of oligomers of length three or shorter. It is important to realize, as shown in Figure 5, that the final product is predicted to contain a significant amount of oligomers (mainly macromonomer) of these lengths. This new population of chains is produced via the CCT mechanism, but do not grow to significant length due to the presence of both Cu and Co transfer agent in the system. Experimentally, these chains are removed from the final material in the precipitation/polymer isolation procedures; when their contribution is removed from the simulated MMDs, there is no change in M_n with the addition of CCT, and the oligomers do not contribute to the predicted level of functionality measured by NMR (as shown in Figure 4d). However, in a previous study of sequential ATRP-CCTP to produce PMMA, the appearance of a small separate

peak in MMDs in the SEC trace of non-precipitated sample was noted (M_n = 390 Da), with subsequent analysis by ^{1}H NMR revealing that the low MW material contained unsaturated end groups.[12]

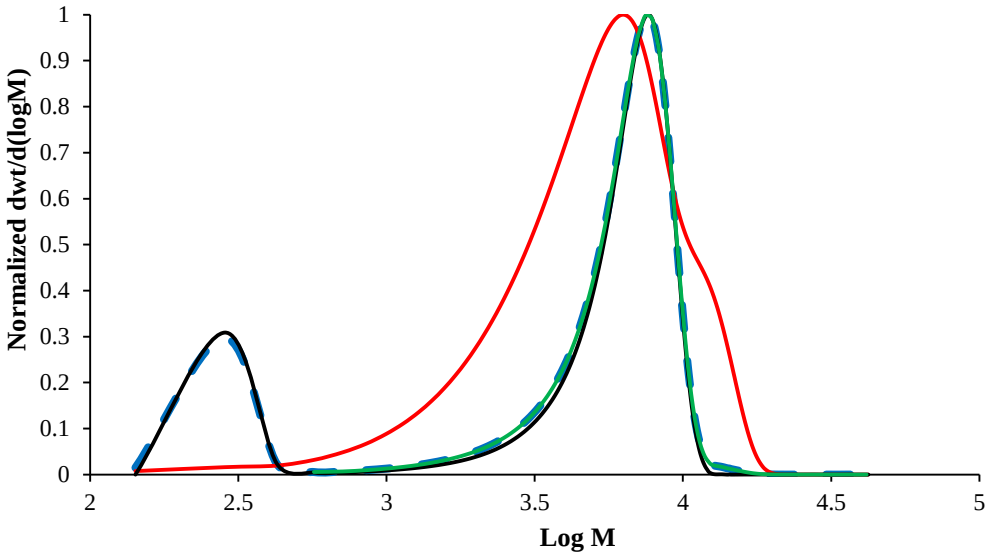

Figure 5. Simulated molar mass distributions of poly(BMA) produced by sequential ATRP-CCTP. Total product distribution shown with (dashed blue) and without (green) the contribution of low MW oligomers. All distributions normalized to a height of 1, with macromonomer chains (black) contributing 90.3 wt% and polymer without vinyl endgroups (red) contributing 9.7 wt% of the total polymer. Simulation for sequential ATRP of BMA with $[M]_0$:$[I]_0$:$[CuBr]_0$:$[L]_0$ = 42:1:0.4:0.8 in 50 wt% anisole at 70 ℃ and 44.8 mg of CoPheBF added at 7200 s. Kinetic parameters for simulation are given in Table 1.

In addition, Figure 5 indicates a significant shoulder at higher molar masses in the MMD of polymer without vinyl endgroups compared to the MMD of the macromonomer. Although providing only a minor contribution to the combined MMD (and thus not greatly increasing dispersity), it is consistent with the experimental observation that the longer chains of the final product are less likely to be functionalized.

Further features of the simulation are provided in the MMDs plotted as Figure 6. As shown by Figure 6a, bromine-capped chains are the main component of the overall distribution as it exists before the CCT addition at 7200 s. However, the high MW shoulder caused by termination by

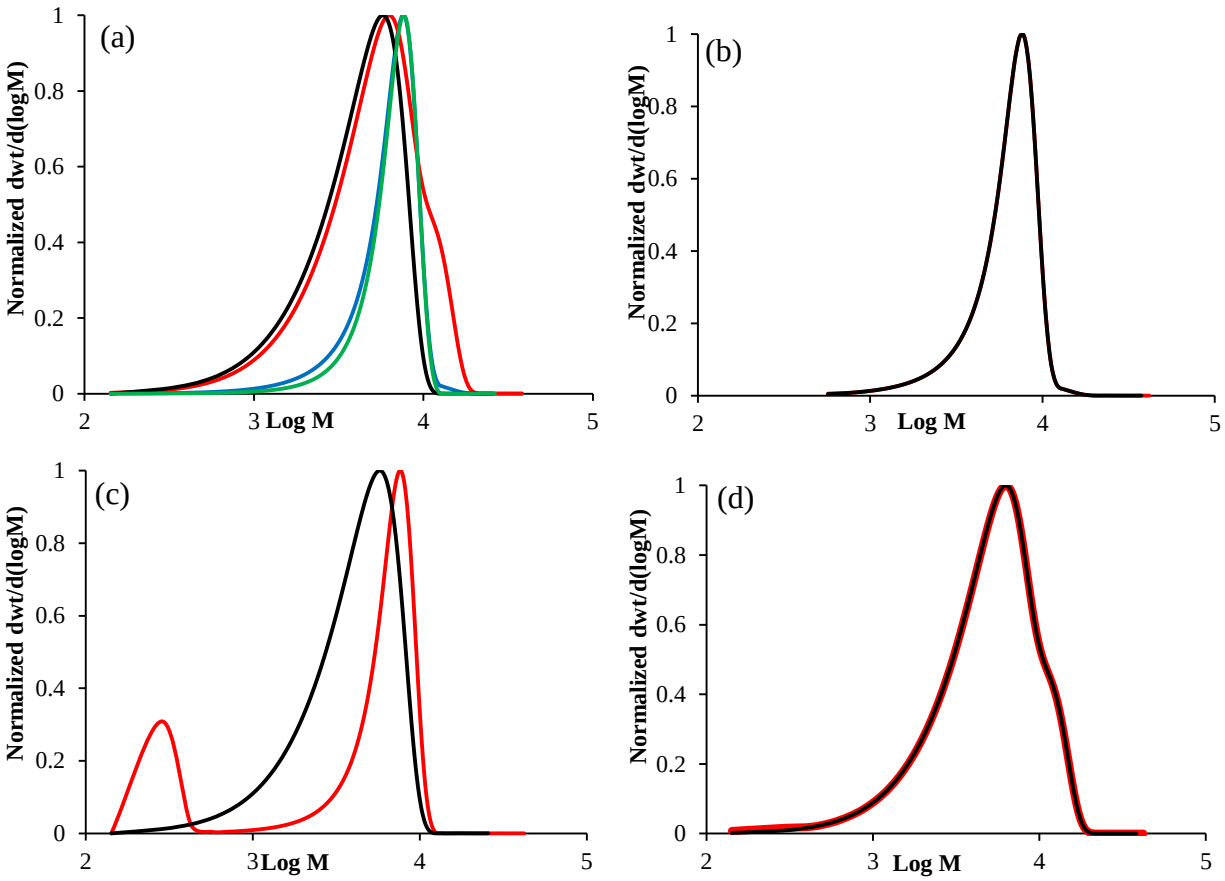

Figure 6. Simulated molar mass distributions (normalized to a height of 1) of (a) total distribution (blue) before the addition of CCT agent at 7200 s (blue) consisting of bromine-capped chains (green, 84.2 wt%), dead chains (red, 9.9 wt%), macromonomer (black, 5.9 wt%); (b) final product without oligomer at 14400 s (red) compared to distribution before CCT addition at 7200 s (black, an exact overlay); (c) macromonomer (with oligomer) at 14400 s (red) and before CCT addition at 7200 s (black); and (d) dead chains at 14400 s (red) and before CCT addition at 7200 s (black). Kinetic parameters for simulation are given in Table 1.

combination is evident in the distribution of dead chains at that time, suggesting that its contribution to the final product MMD can be reduced by manipulation of ATRP operating conditions. Note that the contribution of oligomers with 1 to 3 units in the ATRP-regulated material at 7200 s before the addition of the CCT is negligible, in contrast to the results after CCT addition shown in Figure 5. After addition of CCT agent, the ATRP-mediated living polymer chains are quickly transformed to macromonomers of the same length, with the new radicals formed from the transfer process also quickly converting to form oligomeric macromonomer; as seen in Figure 6b, the MMD of the final

product at 14400 s (after subtracting out oligomeric contributions) is identical to that simulated at 7200 s. However, there is a significant shift and narrowing of the MMD of the macromonomer component from 7200 s to 14400 s (Figure 6c), as the Br-capped chains are converted to macromonomer. Finally, as shown in Figure 6d, the addition of CCT agent does not affect the MMD of the dead chains, confirming that this material is produced during the ATRP portion of the synthesis before addition of the CCT agent. Thus, suppressing the termination that occurs during ATRP is the critical requirement to increasing functionality of the system, including reducing the fraction of long chains without vinyl endgroups produced by termination by combination.

3.3 Effect of CCT Agent Addition Time

As the model provides a reasonable representation of the experimental results, it can be used to explore how the synthesis conditions might be modified to improve the extent of functionalization achieved. The effects of varying the time at which the CCT agent is injected to the ATRP system are shown in Figure 7. While adding the CCT agent earlier in the reaction (at 5400 s, compared to 7200 and 9000 s) leads to a slightly higher conversion (Figure 7a), it has no observable effect on the polymer average molar mass or dispersity (Figure 7b and 7c), or the fraction of chains that have TDB functionality (Figure 7d). This result arises from the fact that these quantities are calculated after subtracting out the contributions of the oligomeric chains of length 3 or shorter; as shown in Figure 7e, these oligomeric chains accumulate in larger quantities when the time of the injection is earlier. Thus, delaying the injection of CCT to later time reduces the amount of monomer that is lost to oligomerization, increasing the yield of usable macromonomer produced. The accompanying drawback is a corresponding slight increase in the fraction of non-functional material produced by termination by combination, as indicated by the increased contribution of the high molecular weight shoulder.

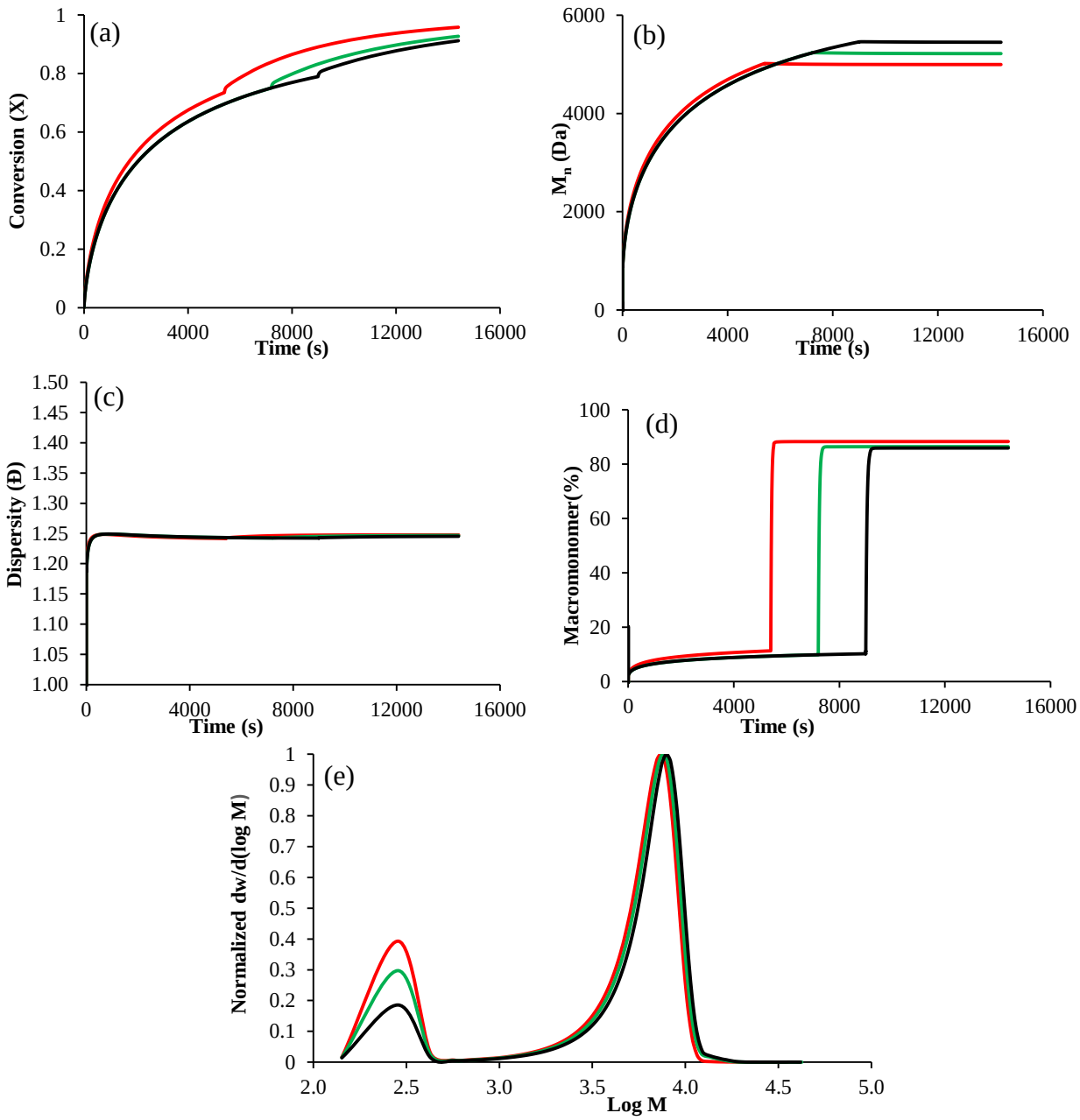

Figure 7. The simulated effect of the CoPheBF addition time from 5400 s (red), to 7200 s (green), to 9000 s (black) on (a) conversion, (b) number average molar mass M_n, (c) dispersity Đ, and (d) % macromonomer profiles, and (e) MMDs of final product (normalized to a height of 1 and including oligomer contributions) produced by sequential ATRP of BMA with $[M]_0$:$[I]_0$:$[CuBr]_0$:$[L]_0$ = 42:1:0.4:0.8 in 50 wt% anisole at 70 ℃. The CoPheBF (44.8 mg) is added at different time and simulation is stopped at 14400 s. Kinetic parameters for simulation are given in Table 1.

4. Conclusions

A mechanistic model of sequential ATRP-CCTP of BMA in anisole at 70 ℃ using Cu(I)Br/PMDETA as the catalyst and EBiB as the ATRP initiator has been formulated. Experimental results are used to estimate $k_{da,0}$, k_a and k_{da} within the range of literature values by fitting the available experimental data using Predici® software. Using literature kinetic parameters to describe CCTP of BMA using CoPheBF, the simulation of the ATRP-CCTP process well describes the experimental results.

The model was used to demonstrate that, as long as the CCT agent is added towards the end of reaction (after 1.5-2.5 h, corresponding to conversions between 70%-85%), it successfully works as a chain terminator to produce the desired macromonomer chains, with any new chains that are produced remaining as oligomeric material (macromonomer with lengths of 1-3 units). A small fraction of polymer chains are produced without vinyl endgroups by termination by combination during the ATRP reaction before the addition of CCT agent; many are of longer length, in agreement with observations made when utilizing the ATRP-CCTP synthesized macromonomer as a dispersant for non-aqueous dispersion polymerization.[8] Finally, simulations indicate that delaying addition of the CCT agent should produce polymer with higher molar mass and a lowered amount of oligomers, improving monomer usage.

Acknowledgement: The authors acknowledge the valuable support from Dr. Jeffery Johnson and Dr. Andrew Stamegna of Axalta Coating Systems (Wilmington, U.S.A), and the funding from Axalta Coating Systems (Wilmington, U.S.A) and the Natural Sciences and Engineering Research Council of Canada.

Keywords: Low Đ macromonomer; ATRP, Cobalt chain transfer polymerization, modeling and simulation, radical polymerization

References

[1] K. G. Suddaby, D. M. Haddleton, J. J. Hastings, S. N. Richards, J.P. O'Donnell, *Macromolecules* **1996**, *29*, 8083.

[2] J. Huybrechts, P. Bruylants, K. Kirshenbaum, J. Vrana, J. Snuparek, *Prog. Org. Coat*. **2002**, *45*, 173.

[3] G. C. Sanders, R. Duchateau, C. Y. Lin, M. L. Coote, J. P. Heuts, *Macromolecules* **2012**, *45*, 5923.

[4] L. M. Muratore, T. P. Davis, *J. Polym. Sci. Pol. Chem.* **2000**, *38*, 810.

[5] W. Yang, R. A. Hutchinson, *Macromol. React. Eng*. **2016**, *10*, 71.

[6] W. Yang, R. A. Hutchinson, *React. Funct. Polym*. **2017**, *114*, 31.

[7] M. Zhang, R. A. Hutchinson, *Macromol. React. Eng*. **2018**, 1800025.

[8] M. Zhang, R. A. Hutchinson, *Macromolecules* **2018**, *51*, 6267.

[9] G. Nurumbetov, N. Engelis, J. Godfrey, R. Hand, A. Anastasaki, A. Simula, V. Nikolaou, D. M. Haddleton, *Polym. Chem*. **2017**, *8*, 1084.

[10] K. Matyjaszewski, J. Xia, *Chem. Rev*. **2001**, *101*, 2921.

[11] K. Matyjaszewski, *Macromolecules* **2012**, *45*, 4015.

[12] J. Norman, S. C. Moratti, A. T. Slark, D. J. Irvine, A. T. Jackson, *Macromolecules* **2002**, *35*, 8954.

[13] J. F. Lutz, K. Matyjaszewski, *J. Polym. Sci. Part A Polym. Chem*. **2005**, *43*, 897.

[14] J. F. Lutz, K. Matyjaszewski, *Macromol. Chem. Phys*. **2002**, *203*, 1385.

[15] Y. Fu, A. Mirzaei, M. F. Cunningham, R. A. Hutchinson, *Macromol. React Eng*. **2007**, *1*, 425.

[16] O. Delgadillo-Velázquez, E. Vivaldo-Lima, I. A. Quintero-Ortega, S. Zhu, *AIChE J.* **2002**, *48*, 2597.

[17] C. Toloza Porras, D. R. D'hooge, P. H. Van Steenberge, M.-F. Reyniers, G. B. Marin, *Ind. Eng. Chem. Res.* **2014**, *53*, 9674.

[18] E. Mastan, S. Zhu, *Eur. Polym. J.* **2015**, *68*, 139.

[19] Y. Fu, M. F. Cunningham, R. A. Hutchinson, *Macromol. Symp*. **2007**, *259*, 151.

[20] Y. Zhou, Z. Luo, *Macromol. React. Eng*. **2016**, *10*, 516.

[21] K. Matyjaszewski, J. Wang, *J. Am. Chem. Soc*. **1995**, *117*, 5614.

[22] M. Sawamoto, M. Kato, M. Kamigaito, T. Higashimura, *Macromolecules* **1995**, *28*, 1721.

[23] K. Matyjaszewski, M. Wei, J. Xia, N. E. McDermott, *Macromolecules* **1997**, *30*, 8161.

[24] W. Tang, N. V. Tsarevsky, K. Matyjaszewski, *J. Am. Chem. Soc.* **2006**, *128*, 1598.

[25] W. Jakubowski, K Matyjaszewski, *Angew. Chem. Int. Ed.* **2006**, *45*, 4482.

[26] X. Li, W. Wang, B. Li, S. Zhu, *Macromol. React. Eng*. **2011**, *5*, 467.

[27] K. A. Payne, D. R. D'hooge, P. H. Van Steenberge, M. Reyniers, M. F. Cunningham, R. A. Hutchinson, G. B. Marin, *Macromolecules* **2013**, *46*, 3828.

[28] G. E. Roberts, C. Barner-Kowollik, T. P. Davis, J. P. Heuts, *Macromolecules* **2003**, *36*, 1054.

[29] D. J. Forster, J. P. Heuts, F. P. Lucien, T. P. Davis, *Macromolecules* **1999,** *32*, 5514.

[30] C. Kowollik, T. P. Davis, *J. Polym. Sci. Part A Polym. Chem.* **2000**, *38*, 3303.

[31] B. Pierik, D. Masclee, A. M. van Herk, *Macromol. Symp*. **2001**, *165*, 19.

[32] A. N. Nikitin, M. C. Grady, G. A. Kalfas, R. A. Hutchinson, *Macromol. React. Eng*. **2008**, *2*, 422.

[33] A. A. Gridnev, S. D. Ittel, B. B. Wayland, M. Fryd, *Organometallics* **1996**, *15*, 5116.

[34] R. A. Hutchinson, S. Beuermann, D. A. Paquet, J. H. McMinn, *Macromolecules* **1997,** *30*, 3490.

[35] A. K. Nanda, K. Matyjaszewski, *Macromolecules* **2003**, *36*, 8222.

[36] W. Tang, K. Matyjaszewski, *Macromolecules* **2007**, *40*, 1858.

[37] F. Seeliger, K. Matyjaszewski, *Macromolecules* **2009**, *42*, 6050.

[38] W. Tang, K. Yungwan, W. Braunecker, N. V. Tsarevsky, M. L. Coote, K. Matyjaszewski, *J. Am. Chem. Soc*. **2008**, *130*, 10702.

[39] K. A. Payne, P. H. Van Steenberge, D. R. D'hooge, M. Reyniers, G. B. Marin, R. A. Hutchinson, M. F. Cunningham, *Polym. Int*. **2014**, *63*, 848.

[40] M. Buback, J. Morick, *Macromol. Chem. Phys*. **2010**, *211*, 2154.

[41] W. Wang, M. C. Grady, R. A. Hutchinson, *Ind. Eng. Chem. Res.* **2009**, *48*, 4810.

[42] J. E. Schier, M. Zhang, M. C. Grady, R. A. Hutchinson, *Macromol. React. Eng*. **2018**, *12*, 1800008.

For Table of Contents

Modeling the synthesis of Butyl Methacrylate Macromonomer by Sequential ATRP-CCTP

*Mingmin Zhang, Robin A. Hutchinson**

M. Zhang, Prof. R. A. Hutchinson
Department of Chemical Engineering, Queen's University,
19 Division St., Dupuis Hall, Kingston, Ontario, K7L 3N6, Canada
E-mail: robin.hutchinson@queensu.ca

After sequential ATRP-CCTP of BMA, the final product (blue) principally consists of macromonomer (black dashed, 90.3 wt%) with a small fraction of polymer without vinyl endgroup (red line, 9.7 wt%). The low molecular weight shoulder consists of macromonomer oligomers formed after addition of the CCT agent.

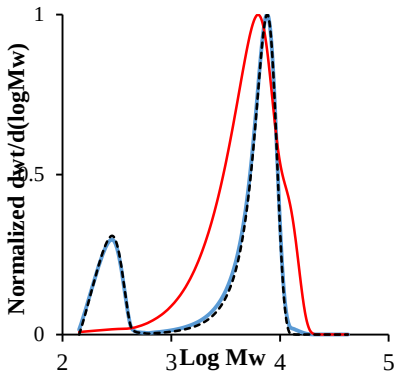

production data